JCTC Journal of Chemical Theory and Computation

Article

pubs.acs.org/JCTC

van der Waals Interaction Energies of Small Fragments of P, As, Sb, S, Se, and Te: Comparison of Complete Basis Set Limit CCSD(T) and DFT with Approximate Dispersion

Ján Brndiar and Ivan Štich*

Center for Computational Materials Science, Institute of Physics, Slovak Academy of Sciences, 84511 Bratislava, Slovakia

Supporting Information

ABSTRACT: Interaction energies of small model van der Waals fragments of group VA (P, As, Sb) and group VIA (S, Se, Te) are calculated using the complete basis set CCSD(T) method and compared to density functional results with approximate treatment of dispersion interaction using vdW-DF- and DFT-D-types of theories. These simple systems show surprising diversity of electronic properties ranging from more "metallic" to more "insulator" like, a property which needs to be captured in the approximate methods. While none of the standard approximate DFT theories provides an entirely satisfactory description of all the systems, we identify the most reliable approaches of each type. In addition, we show that results can be further tuned to chemical accuracy. In vdW-DF theory, guided by physical insights and the availability of quasi-exact CCSD(T) results, we supply the missing parts of correlation by matching an appropriate hybrid/semilocal exchange-correlation functional to describe short-/medium-range correlations accurately. In the DFT-D-type of theories, we reparametrize the empirical dispersion term. Since for such an accurate treatment benchmark calculations are needed, which typically is feasible only for a finite cluster, we argue that the cluster based model of the exchange-correlation hole is transferrable also to extended systems with vdW dispersion interactions.

1. INTRODUCTION

Noncovalent interactions, such as van der Waals (vdW) or hydrogen bonding, are among the most important interactions. They are responsible for the existence of sparse condensed matter from the formation of graphite and molecular crystals to double strands of DNA.[1] Modeling of the physics and chemistry of London dispersion interactions[1] may appear straightforward due to the simple C_6R^{-6} form, but in reality the vdW interaction is a quantum-mechanical phenomenon correlating electromagnetically charge fluctuations in one part of the system to charge fluctuations in another part and, hence, is a *nonlocal correlation effect*.

In this paper, we focus on a special class of group VA and VIA systems formed from covalently bonded fragments held together predominantly by vdW interactions. Examples being extended condensed systems such as white phosphorus, yellow arsenic, the S_6 bulk structure of sulfur, or rhombohedral selenium composed of Se_6 fragments. Surprisingly, very little attention has been paid to these systems despite the fact that some of them, such as, for instance, antimony, form an important class of vdW bonded systems and interfaces often used in nanotribology.[2,3] Nanotribology is a very stringent test, as the spacer molecules locking the interfaces[2,3] will explore the potential energy surfaces (PES) also far from the minima. A similar situation will arise also when dynamics of vdW systems or vdW systems under pressure are studied. Hence, in all of these cases, a high accuracy description of the entire PES is needed. We provide here such a study for a class of model vdW fragments of VA and VIA groups and argue that an approach based on a cluster description of electronic correlations on all length scales is transferrable also to extended systems. These results fill an important gap in understanding vdW interaction. This is at variance with other vdW systems, such as, for instance, the well studied S22 set[4−6] and other chemistry sets[7−9] or organic molecules on surfaces[10,11] where extensive comparison studies exist.

Only a few methods, namely high-level quantum chemistry and quantum Monte Carlo (QMC) methods, are able to directly account for the vdW interaction, while the popular density functional (DFT) methods in local (spin) density (LDA/LSDA) and generalized gradient correction (GGA) approximations fail to account for the correct long-range interaction tail. The selection of techniques we use to add the missing correlation, E_{Disp}, to the ordinary Kohn−Sham DFT energy

$$E_{\mathrm{DFT-Disp}} = E_{\mathrm{DFT-KS}} + E_{\mathrm{Disp}} \quad (1)$$

is briefly summarized below. A basic assumption behind such a partitioning is that short-, medium-, and long-range electronic correlation effects operate on different, well separated, length scales. This, though, is not entirely true. Overlap of different correlations at midrange can cause ambiguities, and proper matching of correlations at different length-scales is the key to achieving high accuracy. Moreover, common functionals such as PBE, TPSS, or B3LYP, which perform well for many important properties, may not be optimal for noncovalent interactions.[12,13] Comparison studies of the different techniques designed to capture dispersion interactions are relatively rare. Hence, revealing their merits, drawbacks, and routes for their

Received: March 30, 2012
Published: June 14, 2012

 © 2012 American Chemical Society

improvement is another important objective of the present study.

Langreth, Lundqvist, and collaborators suggested *van der Waals DFT* (vdW-DF) theory[14,15] with a fully *nonlocal functional*, $E_c^{nl}[n]$, of the charge density n correlated via the kernel ϕ

$$E_{Disp} = E_c^{nl}[n] = \int d^3r \int d^3r'\, n(\mathbf{r})\, \phi(\mathbf{r}, \mathbf{r}')\, n(\mathbf{r}') \quad (2)$$

called vdW-DF1,[14] later slightly improved to vdW-DF2.[15] In vdW-DF theories, the kernel ϕ uses different approximations to the plasmon-pole model.[14,15] In fact, the dispersion formula used in the dielectric function describes also the rest of the mid- and short-range part of the exchange-correlation (xc) hole ($E_{xc}^0 = E_{xc} - E_c^{nl}$) and, hence, the entire xc hole.[16] Alternatively, E_{xc}^0 can be used to tune the results by adding the missing part of short-/medium-range correlations. For example, vdW-DF2 theory chooses $E_{xc}^0 = E_x^{rPW86} + E_c^{LDA}$. The argument behind this choice is that the use of reparametrized rPW86 exchange[17,18] with an appropriate enhancement factor gives the most consistent agreement with Hartree−Fock results, without spurious exchange binding, while use of LDA correlation precludes double counting. Alternative modifications of the exchange term were suggested by Klimeš et al.[19] However, Vydrov and Van Voorhis noticed that existing vdW-DF theories will, in general, need also semilocal gradient correlation (GC) corrections.[20] Such a choice is made in the recent (VV10) version[20] of the *Vydrov Van Voorhis van der Waals* (VV-vdW) theory,[16,20,21] which adds the PBE type of GC correction, $E_{xc}^0 = E_x^{rPW86} + E_c^{PBE}$. In addition, VV10 also uses a different approximation to the plasmon-pole model. VV10 VV-vdW theory is not free of fitting parameters in merging the E_c^{nl} and E_{xc}^0, which are fixed by fitting the S22 set.[5] For other classes of systems, different benchmark sets could be used. Alternatively, based on a given benchmark chosen, the missing correlations and/or exchange could be directly added to the model of E_{xc}^0, a strategy we follow here in connection with vdW-DF theory. vdW-DF is especially well suited to this purpose as there is no fitting involved and both E_{xc}^0 and E_c^{nl} are consistently treated. The challenge here is to recognize if correlation, exchange, or both need to be amended. Intuitive tools will be introduced in section 3. As shown below, in this way E_{xc}^0 can be tuned to achieve chemical or better accuracy (1 kcal/mol or 0.04 eV) for the interaction energy, E_{int}.

A radically different approach was suggested by Grimme et al.[12,22−24] in the *DFT-D*-type of theory, which proposes a direct two-body correction of the form

$$E_{Disp} = \sum_{A,B} \sum_{n=6,8,10,...} s_n \frac{C_n^{AB}}{r_{AB}^n} f_{dmp}^{(n)}(r_{AB})$$

$$f_{dmp}^{(n)}(r_{AB}) = \frac{1}{1 + 6(r_{AB}/(s_{r,n} R_0^{AB}))^{-\alpha_n}} \quad (3)$$

with s_n being a scaling factor and $f_{dmp}^{(n)}(r_{AB})$ a damping factor. In contrast to the vdW-DF theories, the damping factor helps to directly decouple the long-range nonlocal correlations from the medium-/short-range correlations and, hence, makes them easier to handle accurately. A special bonus is the computational efficiency compared to vdW-DF theories. However, compared to the vdW-DF theories, such an approach is not ab initio. In the early DFT-D1/D2 formulations,[22,23] only empirically determined C_6 terms were considered. In the recent DFT-D3 formulation,[12] in addition to C_6 also the C_8 term is considered with the atomic dispersion coefficients determined from time-dependent DFT theory (TDDFT). The other important feature is the fact that the dispersion coefficients are made *geometry dependent* without the need to compute them from electronic structure calculation. However, depending on the system, use of TDDFT for dispersion coefficients in connection with the damping functions which require fitting of further scaling parameters s_n and $s_{r,n}$ in eq 3 may result in biases. To describe the short-/medium range xc hole, E_{xc}^0, B97[25] or TPSS[26,27] functionals are frequently used.

The problem of an accurate determination of system dependent dispersion coefficients was addressed by Tkatchenko and Scheffler,[28] who proposed a simple procedure for estimating the C_6 dispersion coefficient and vdW radius of an atom R_r in a DFT-D-type of approach inside a molecule or solid by a Hirshfeld partitioning of the total electron density:

$$C_{6A}^{eff} \approx \left(\frac{V_A^{eff}}{V_A^{free}}\right)^2 C_{6A}^{free} = \left(\frac{\int r^3\, w_A(\mathbf{r})\, n(\mathbf{r})\, d^3r}{\int r^3\, n_A^{free}(\mathbf{r})\, d^3r}\right)^2 C_{6A}^{free}$$

$$w_A(\mathbf{r}) = \frac{n_A^{free}(\mathbf{r})}{\sum_B n_B^{free}(\mathbf{r})}$$

$$E_{Disp} = -s_6 \sum_{A,B} \frac{C_{6AB}}{r_{AB}^6} f_{dmp}(r_{AB})$$

$$f_{dmp}(r_{AB}) = \frac{1}{1 + \exp(-d(r_{AB}/s_r R_r^{eff} - 1))}$$

$$R_r^{eff} = \left(\frac{V_A^{eff}}{V_A^{free}}\right)^{1/3} R_r^{free} \quad (4)$$

where $w_A(\mathbf{r})$ is the Hirshfeld atomic partitioning weight for atom A, $n(\mathbf{r})/n_A^{free}(\mathbf{r})$ is the total/atom A DFT determined electron density, and C_{6A}^{free}/R_r^{free} is an accurate dispersion coefficient/vdW radius of an atom, which may be determined by a reference method. Equation 4 proposes the use of C_{6A}^{eff} in a simplified DFT-D2-type of dispersion energy, E_{Disp}, with a Fermi-type damping function $f_{dmp}(r_{AB})$. We note in passing that the form of the damping function f_{dmp} in eqs 4 and 3 is different. The Tkatchenko−Scheffler method is most frequently used with PBE,[29,30] PBE0,[31,32] or HSE[33] functionals to describe the short-/medium-range xc effects,[6] E_{xc}^0. Scheffler et al. have also shown that many-body collective response in a solid[34] or on a substrate[35] can lead to screening of the vdW interactions, which can be accounted for by use of a dielectric function.[34,35]

The paper has more objectives. (1) We form a benchmark database of vdW interactions between small fragments which form the structural motives of the molecular crystals of the series of P, As, Sb, S, Se, and Te crystal structures. The fragments considered are depicted in Figure 1. They consist of pairs of interacting tetrahedra in P, As, and Sb and pairs of 6-fold buckled rings in S, Se, and Te. Our approach is in spirit very similar to that adopted by Hobza et al. for biomacromolecules like DNA, RNA, and proteins[4,5] and by Deligkarisz and Rodriguez for biomolecular systems described by their B3LYP-DD method.[36] The fragments are small enough

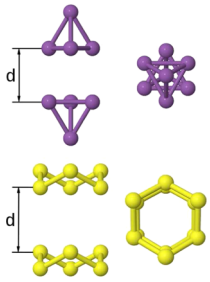

Figure 1. Fragments considered for study as models of vdW interaction in P, As, and Sb (upper panels, pink color) and in S, Se, and Te (lower panel, yellow color). d is the distance between fragments allowed to change. For details, see the text.

to be practical for high-level quantum chemistry treatment, such as the complete basis set (CBS) limit of CCSD(T).[5] This is very important as to the best of our knowledge the exact results for these and similar systems are not known. (2) These quasi-exact results are then used for a comparison study of the different approximate approaches outlined in eqs 1−4. Such a study yields an important contribution to validation of the methods for approximate treatment of the dispersion interactions in systems so far outside of the validation scope. Indeed, we find systematic trends in the quality of the description of the dispersion interaction which can be used either for selection of the most accurate approximate treatment of vdW interaction or for improvement or reparametrization of the existing methods. Our results indicate that when truly accurate results with chemical or better accuracy are required for calculations where a wide range of the PES will be sampled, an appropriate treatment can be based on the accurate treatment of small clusters mimicking the extended systems, which are small enough to allow their treatment either by correlated quantum chemistry or by quantum Monte Carlo methods and large enough to correctly describe the xc hole in the extended system. (3) These results can subsequently be used to select the most accurate mix of DFT xc functionals and a description of dispersion interaction. (4) Due to a rapid convergence of the short-/medium-range xc hole and energy (E_{xc}^0) with the cluster size,[37] these results, after correcting the vdW terms for possible screening effects,[34,35] are then transferable to the extended systems.

2. METHODS

We have calculated interaction energy curves for the structural models shown in Figure 1 for P, As, Sb, S, Se, and Te. The structures for P, As, and Sb fragments were symmetry constrained to D_{3d} and allowed to relax at each fixed distance between the bases of the tetrahedra. Symmetry constraints served mainly to reduce the number of degrees of freedom in the CCSD(T) geometry optimization. For S, Se, and Te fragments, the structures showed only little propensity to relaxation, and hence, the energy-distance curves were calculated as single point D_{3d} symmetry constrained energies for individually relaxed S, Se, and Te fragments. Each curve was calculated with both quantum chemistry (CBS CCSD(T)) and DFT methods (vdW-DF2, VV-vdW, DFT-D2, DFT-D3, and DFT-D2 with the dispersion constant C_6 and R_r^{eff} determined from eq 4 labeled as DFT-D2 HP). Initially, DFT-D2/D3 calculations were coupled with the TPSS functional to describe short-/medium-range xc effects, while DFT-D2 HP calculations were coupled with the PBE xc functional, see section 1. However, we found that both PBE and TPSS functionals produce spurious exchange binding[14,18] for group VA fragments, see section 3. Therefore, the revPBE xc functional was used for group VA, and TPSS/PBE functionals were used for group VIA. For other couplings, see the Supporting Information (SI). In addition, in vdW-DF2, the effect of exact, i.e., Hartree−Fock (HF), exchange (vdW-DF2 HF) and PW91 semilocal GC correction[38] (vdW-DF2 GC) on E_{xc}^0 have been tested with the quest to design the most accurate E_{xc}^0/E_{xc}^{nl} coupling. Due to the empirical character of E_{Disp} in DFT-D2/D3 techniques, E_{xc}^0 was modeled only in the PBE/revPBE/TPSS approach. In the Tkatchenko−Scheffler method[28] (DFT-D2 HP), the parameters of the damping function $f_{dmp}(r_{AB})$ can be optimized for our system set (labeled DFT-D2 HPF). Indeed, we have calculated the C_6 dispersion coefficients using the Tkatchenko−Scheffler method in the DFT-D2-type of approach and reparametrized the s_6/s_r parameters in order to fit our CBS CCSD(T) results. In addition, in order to determine the CBS CCSD(T), we have also considered CBS MP2 curves computed at CCSD(T) geometries. Together, nine different determinations of the interaction curves have been made for each system, see the SI for results with complementary E_{xc}^0/E_{Disp} couplings. All calculated points were fitted with the Morse formula. Technical details of each type of calculation are briefly summarized below.

Quantum Chemistry. *CCSD(T)* geometry optimization was performed using energy-consistent pseudopotentials[39] with the accompanying cc-pVTZ Dunning-type basis sets[40] and the GAMESS suite of codes.[41] The HF and correlation interaction energies were corrected for the basis set superposition error (BSSE).[42] The CBS limit of CCSD(T) was determined[5] by

$$E_{\text{CBS}}^{\text{CCSD(T)}} = E_{CBS}^{MP2} + (E^{\text{CCSD(T)}} - E^{\text{MP2}})_{\text{SBS}} \quad (5)$$

with SBS labeling small basis set result and $E_{\text{CBS}}^{\text{MP2}}$ determined from[43,44]

$$E_X^{\text{HF}} = E_{\text{CBS}}^{\text{HF}} + BX^{-\alpha} \text{ and } E_X^{\text{corr}} = E_{\text{CBS}}^{\text{corr}} + BX^{-\beta} \quad (6)$$

in which E_X is the energy for the basis set with the largest angular momentum X. Five different basis set were used, T, Q, T^-, Q^-, and 5^-, with N^- labeling the basis set with highest angular momentum channel removed. This choice was motivated by (1) disregarding D basis sets[5] and (2) the limitation of the GAMESS code to g angular momentum. The CBS limit of CCSD(T) was calculated for P and S using the energy consistent pseudopotentials and basis sets,[39] while using the correlation consistent (cc-pVXZ)[40] basis set and effective core pseudopotentials (ECP)[45] for the other elements. An example of convergence properties of the CBS limit is summarized for P_4−P_4 fragments at the CCSD(T) energy minimum in Table 1; the convergence at other distances and for other systems is qualitatively similar. The many-body contribution $(E^{\text{CCSD(T)}}-E^{\text{MP2}})_{\text{SBS}}$ is converged with accuracy better than ∼7 meV at the cc-pVTZ level, see Table 1. The

Table 1. Convergence of Interaction Energies (in meV) with Respect to the Basis Set for the P_4−P_4 Fragments at the CCSD(T) Energy Minimum

basis set	D	T^-	T	Q^-	Q	5^-
MP2	−152	−239	−251	−298	−301	−319
CCSD(T)	−37		−112		−155	
CCSD(T) - MP2	115		139		146	

dx.doi.org/10.1021/ct300258z | J. Chem. Theory Comput. 2012, 8, 2301−2309

MP2 convergence with respect to the removed highest angular momentum channel in the basis set is complete at the 5^- level, see Table 1; hence we construct the CBS limit from the *T*, *Q*, and 5^- combination. We estimate that our CBS limit is converged to an accuracy better than ∼20 meV.

DFT-*D2/3* calculations[12,23] have been performed in the framework of a plane wave pseudopotential formalism[46] with ultrasoft pseudopotentials[47] at a plane wave cutoff of 40 Ry using the PBE/revPBE/TPSS xc functionals[26,27,29,30,48] and the CPMD code.[49] The same code was also used to compute the dispersion coefficients from eq 4.

DFT *vdW-DF2* calculations[15] have been done with norm-conserving pseudopotentials[50] at a plane wave cutoff of 100 Ry with the QUANTUM ESPRESSO code,[51] while the VV10 flavors[20] of *VV-vdW* calculations[16,20,21] have been done with ECP pseudopotentials[45] and cc-pVTZ basis sets[40] with the ORCA code.[52]

3. RESULTS AND DISCUSSION

We now turn to a discussion of results obtained as explained in sections 1 and 2 and discuss separately the Sb−P and Te−S series of fragments.

Results for the **group VA** *Sb−P series of fragments* are shown in Figures 2, 3, and 4; values of the equilibrium interaction

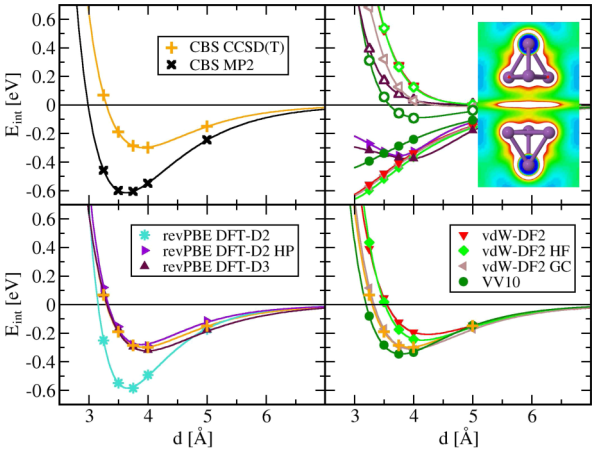

Figure 2. Interaction energies, E_{int}, for Sb_4−Sb_4 fragments as calculated in the complete basis set limit MP2 and CCSD(T) (upper left panel), Grimme's DFT-D2,[23] DFT-D3[12] vdW theory, the DFT-D2-type of treatment with Tkatchenko−Scheffler[28] determination of the C_6 dispersion coefficients (DFT-D2 HP; lower left panel), Langreth−Lungqvist vdW-DF2 theory, vdW-DF2 with exact exchange (vdW HF), vdW-DF2 with semilocal gradient correlations (vdW GC), and the VV10 flavor of VV-vdW theory[20] (VV10; lower right panel). The upper right panel shows separately $E_{int} - E_c^{nl}/E_{int} - E_{Disp}$ (empty marks) and E_c^{nl}/E_{Disp} (full marks). The inset shows a map of the local gap density $g(\mathbf{r}) \in \langle 0.8, 1.45 \rangle$ for the cluster position near the energy minimum on a plane through the interaction space. Color coding: red, yellow, green, and blue in increasing order. For details see section 1.

energy E_{int} and separation d_{eq} of the fragments are summarized in Table 2 of the SI. As expected, (revPBE/rPW96) DFT results with no added dispersion, i.e., with short-/medium-range E_{xc}^0 only, yield no bonding at all for all three fragments. However, as shown in Figure 5 for the Sb_4−Sb_4 fragment, TPSS and PBE xc functionals both yield spurious exchange binding. Similar, albeit weaker, effects were found also for As_4−As_4 and P_4−P_4 fragments, see the SI. A propensity to spurious exchange binding for the PBE functional was also noticed previously.[14,18]

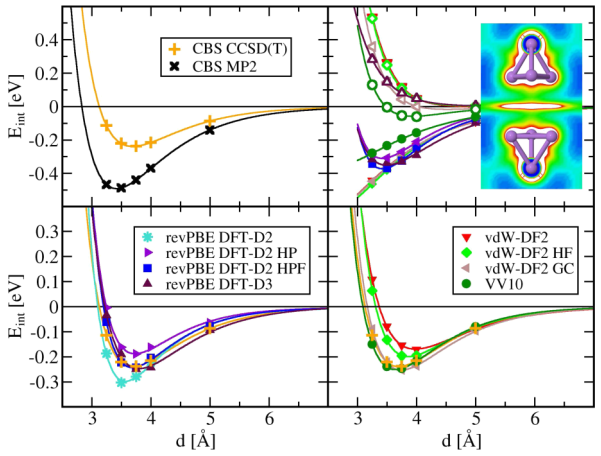

Figure 3. Interaction energies for As_4−As_4 fragments. Caption details as in Figure 2, except for DFT-D2 HPF, which stands for the DFT-D2-type of treatment with Tkatchenko−Scheffler[28] determination of the C_6 dispersion coefficients and modified s_6 and s_r parameters in f_{dmp} in eq 4. For details, see the text.

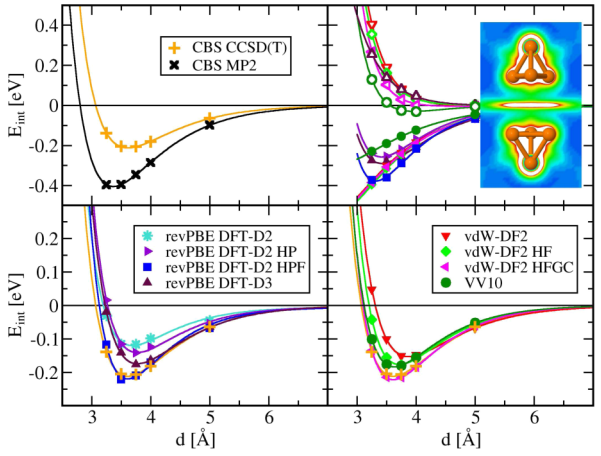

Figure 4. Interaction energies for P_4−P_4 fragments. Caption details as in Figures 2 and 3. vdW-DF2-HFGC stands for vdW-DF2 treatment with E_{xc}^0 calculated with both exact exchange and semilocal correlation corrections.

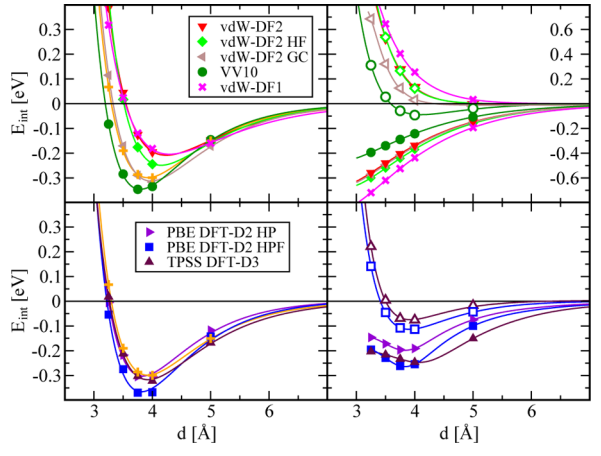

Figure 5. Interaction energies for Sb_4−Sb_4 fragments. Lower panel, DFT-D theories using the TPSS/PBE model of the short-/medium-range xc funcional. Upper panel, results of VV-vdW and vdW-DF theories with different models for E_{xc}^0/E_c^{nl} partitioning. Caption details as in Figures 2 and 3.

dx.doi.org/10.1021/ct300258z | J. Chem. Theory Comput. 2012, 8, 2301−2309

Hence, in order to base our results on a sound description, E_{xc}^{0} in group VA was described with revPBE, which does *not* suffer from such a deficiency.

The CBS CCSD(T) description gives well pronounced minima with interaction energies $E_{int} \approx 200-300$ meV at $d_{eq} \approx 3.6-3.9$ Å. Very clear trends emerge also from the MP2 calculations, which are the opposite of the DFT results in that MP2 is overbinding with $E_{int} \approx 400-600$ meV, about a factor of 2 too large and with the minima at $d_{eq} \approx 3.3-3.6$ Å, about 0.3 Å too small.

vdW−DF2 in its original version underbinds in all three cases ($E_{int} \approx 150-210$ meV, $d_{eq} \approx 3.9-4.2$ Å), i.e., about 30% underbinding with distances about 0.3 Å too large. In addition, in all three cases, E_{xc}^{0} with E_{x}^{rPW86} and E_{c}^{LDA} are too repulsive, compared to CCSD(T). Hence, remedy must come primarily from improvement of the short-/medium-range xc effects. One way of achieving this is by use of hybrid functionals and/or semilocal gradient correlation corrections. To decide which part of E_{xc}^{0} needs amendments, we use the concept of a *local gap*.[54] The amount of HF exchange mixing in a hybrid functional can be related to the *local gap density*[54]

$$g(\mathbf{r}) = \sqrt{|\nabla n(\mathbf{r})|/n(\mathbf{r})} \tag{7}$$

$g(\mathbf{r})$ is small in metallic systems and large in insulating systems, with insulating systems needing more amendment of the exchange than metals. Indeed, the maps of $g(\mathbf{r})$ for Sb and As shown in Figures 2 and 3 show very low values, hence a *metallic* behavior. P, shown in Figure 4, already exhibits an onset of higher $g(\mathbf{r})$ values and, hence, a transition to an *insulating* system. Therefore, we have repeated the calculations with rPW86 exchange replaced by exact HF exchange (vdW-DF2 HF curves). As can be seen from Figures 2 and 3 for Sb and As, the E_{xc}^{0} curves calculated with exact exchange and rPW86 exchange are identical, which is not entirely true for P, see Figure 4. Hence, a semilocal GC correlation correction was added (vdW-DF2-GC curves), which markedly improved agreement with our CCSD(T) benchmarks. We seek a framework flexible enough to account for both missing correlations and faults in DFT exchange. In practice, the procedure we apply comes close to the Becke3LYP hybrid functional;[55] we take

$$E_{xc}^{0Becke3LYP'} = (1 - a_0)E_{x}^{rPW86} + a_0 E_{x}^{HF} + E_{c}^{LSDA} + a_c \Delta E_{c}^{PW91} \tag{8}$$

For Sb and As, we take $a_0 = 0$, and for a_c we found that a value of 0.5 provides a very accurate description in the noncovalent regime. In the more insulator-like P system, a better description is obtained by setting $a_0 = 0.5$ and $a_c = 0.5$ (Figure 4, vdW-DF2-HFGC curve), hence by mixing in also exact exchange due to the more localized nature of the charge density. This rough parametrization could be further improved, if needed.

VV-vdW is significantly more accurate than vdW-DF2. Part of the success is that VV-vdW makes standard use also of semilocal GC corrections,[20] which is not the case in vdW-DF2. However, in all three cases, the addition of a full GC correction results in the formation of a minimum of E_{xc}^{0} around ∼4 Å. This is distinctly different from the spurious exchange binding observed in the PBE/TPSS description of E_{xc}^{0}. We believe that in the regime of noncovalent interaction, the use of $a_c = 1$ is less accurate than the value we use ($a_c = 0.5$), which not only leads to a better agreement with our CCSD(T) benchmarks but also results in an E_{xc}^{0} curve without minima. We conclude that group VA Sb and As systems, and to a lesser degree also the P system are *correlation dominated*, and the missing link in the vdW-DF2, leading to a systematic underbinding, is the semilocal gradient correlation correction.

The trends in the DFT-D-type of description are less clear and more system dependent. Such a behavior is to be expected, given their construction. In the Sb_4-Sb_4 fragments, Figure 2, the DFT-D3 yields almost accurate results with deviations of only a few percent. However, enormous error arises in the more empirical DFT-D2 treatment, which yields results of quality very similar to that of MP2 with a strong tendency to overbinding. The problem can unambiguously be traced to the C_6 dispersion coefficient, see Table 2, as the same treatment with C_6 determined by HP partitioning of the charge density[28] (DFT-D2 HP) fixes the problem to yield a C_6 coefficient more similar to the one found in the DFT-D3 treatment and accordingly an interaction curve of the DFT-D3-type quality. The DFT-D2 C_6 coefficient is clearly too large, as all the other methods reduce the dispersion coefficient in the fragment relative to free atom, whereas DFT-D2 increases C_6 by ∼25% relative to the free atom value.

Table 2. Values of the Dispersion Coefficient C_6 (in a.u.) in Free Atom and in the Fragments Averaged over All Atoms in the Fragment As Calculated in the Different Approaches[a]

group	VA			VIA		
system	Sb_4-Sb_4	As_4-As_4	P_4-P_4	Te_6-Te_6	Se_6-Se_6	S_6-S_6
free atom	492	246	185	445	210	134
DFT-D2	667	284	136	550	219	97
DFT-D2 HP	450	224	163	445	210	134
DFT-D3	418	224	152	418	210	125

[a]All charge densities were obtained in the revPBE approach.[48] Free atom values and DFT-D2 HP treatment use the database of refs 28 and 53.

The situation in the As_4-As_4 system, Figure 3, is very similar albeit less strongly pronounced. Again, DFT-D3 results are very accurate. DFT-D2 overbinds, but only by ∼25%. The results are slightly improved by DFT-D2 HP treatment. That trend follows a similar trend in the C_6 coefficients, see Table 2.

In the P_4-P_4 system, Figure 4, the situation is different in that also the DFT-D3 is somewhat less accurate both in terms of E_{int} and d_{eq}, resulting in underbinding. DFT-D2 underbinds even more strongly, a trend somewhat alleviated by DFT-D2 HP treatment. These trends are again rooted partially in the C_6 coefficients, Table 2. However, as both C_6 coefficients as well as the damping functions f_{dmp} in DFT-D2 HP and D3 treatments are quite similar, we conclude that better results could only be achieved via reparametrization of f_{dmp}, curve DFT-D2 HPF in Figure 4. In DFT-D, the dispersion term, E_{Disp}, is empirically fitted and, hence, most prone to biases. We have increased s_6 by 20% and set s_r to 0.97, see eq 4. Identical reparametrization indeed results in a PES much more accurate around the minimum not only for the P_4-P_4 system but also for the As_4-As_4 system, see Figure 3. The residual discrepancies at small distances could only be fixed by a better description of the short-/medium-range xc hole (E_{xc}^{0}), hence by improving on the revPBE description of E_{xc}^{0}. Similarly, to fix the residual discrepancies at large distances would require modification of the form of f_{dmp}.

It is interesting to compare the different approximations to E_{c}^{nl} from the vdW-DF2/VV-vdW theories with E_{Disp} from the

DFT-D-type of theories, Figures 2, 3, and 4. First, within a given kernel, E_c^{nl} shows only weak dependence on the density used to construct it. A similar statement can be made about E_{Disp} from D2 HP and D3 theories, which can be understood as both sets of C_6 are quite close, see Table 2, and the damping functions are also similar. However, E_c^{nl} and E_{Disp} differ considerably at short-/midrange distances where E_{Disp} has a turning point absent from vdW-DF2/VV-vdW theories, while E_c^{nl} and E_{Disp} are quite similar at large distances. These differences are rooted in the behavior of E_{xc}^0. There are few general trends; curves with rPW86 and exact exchange are very similar and most repulsive. Semilocal gradient correlation corrections decrease the repulsive character. Adding full PW91 GC correction causes even appearance of a minimum of E_{xc}^0. Finally, use of revPBE exchange again change the E_{xc}^0 curve qualitatively. Yet, the final interaction E_{int} curves are much more similar than the E_{xc}^0 curves. This is mainly due to the compensation effect between the two as the final result is fitted to accurate data sets both in DFT-D and VV-vdW theories and vdW-DF theories build E_{xc}^0 and E_c^{nl} consistently with the same approximations. The most striking manifestation of such a behavior is the use of TPSS/PBE E_{xc}^0 curves, which all have a minimum in DFT-D2/D3 theories, see Figure 5 and the SI, to yield final E_{int} curves of similar quality to the ones discussed here. Figure 5 shows also an alternative demonstration that it is the correlation, as opposed to exchange, that accounts for residual errors in the vdW-DF2 description of the fragments in group VA. Figure 5 depicts vdW-DF1 results for Sb_4-Sb_4 fragments. vdW-DF1 uses a different (revPBE) model for exchange and LDA correlations; $E_{xc}^0 = E_x^{revPBE} + E_c^{LDA}$, which is also consistently used to construct the kernel $\phi(r,r')$, eq 2. Both E_{xc}^0 and E_c^{nl} in vdW-DF1 are significantly different separately from vdW-DF2, but E_{int} is indistinguishable in the two models. This provides an independent proof that it is part of the correlation that is missing in vdW-DF theory.

Results for the **group VIA** *Te−S series of fragments* are shown in Figures 6, 7, and 8 with dispersion coefficients C_6 summarized in Table 2 and equilibrium values of E_{int} and d_{eq} in Table 2 of the SI. CBS CCSD(T) interaction curves again have a minimum of ∼200−400 meV at distances of ∼3.3−3.4 Å. CBS MP2 overbinds by a factor of 2−3 with bonding distances being too short (∼3.0 Å) by ∼0.3 Å.

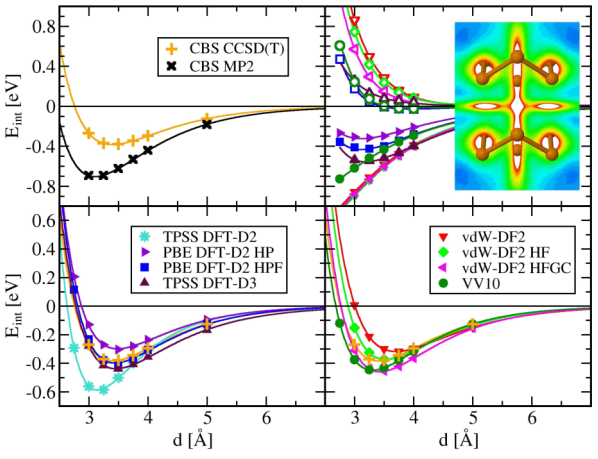

Figure 6. Interaction energies for Te_6-Te_6 fragments. Caption details as in Figures 2 and 3.

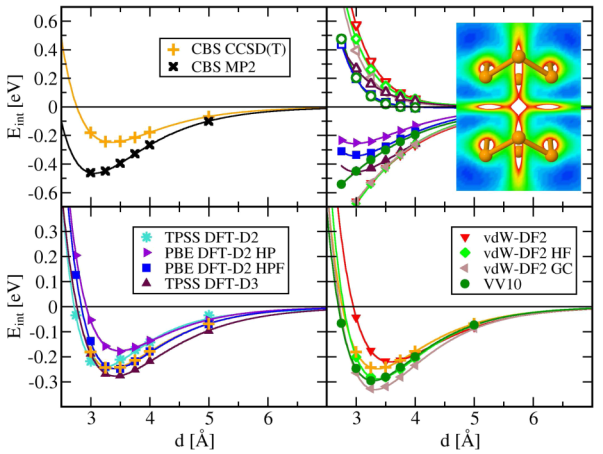

Figure 7. Interaction energies for Se_6-Se_6 fragments. Caption details as in Figures 2 and 3.

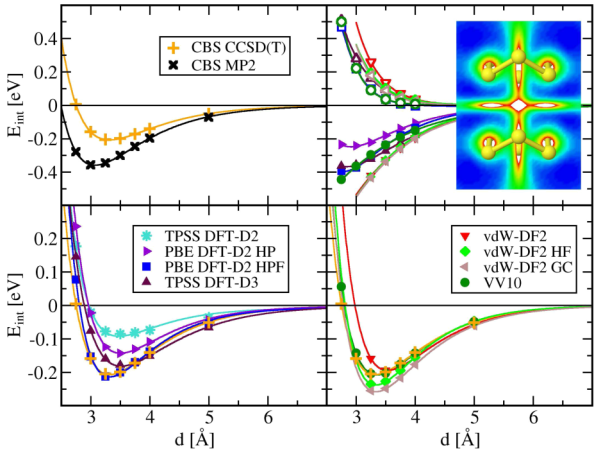

Figure 8. Interaction energies for S_6-S_6 fragments. Caption details as in Figures 2 and 3.

vdW−DF2 in its original version ($E_{xc}^0 = E_x^{rPW86} + E_c^{LDA}$) again underbinds in all three cases ($E_{int} \approx 190-320$ meV, $d_{eq} \approx 3.5-3.9$ Å). E_{xc}^0 in vdW-DF2 was too repulsive in group VA, compared to CCSD(T), and so is also in group VIA. The local gap density $g(\mathbf{r})$ shown in the insets can again provide guidance in the search for improvement of E_{xc}^0. We find that the Te fragments are more *metallic* and, hence, more similar to Sb and As, whereas S and Se are more of the *insulator* type and, hence, closer to P. Therefore, rPW86 exchange replaced by exact HF exchange, Figures 7 and 8, makes E_{xc}^0 less repulsive and indicates that in the interaction in group VIA *exchange* plays a key role. The fact that faults in exchange contribute to the bias in vdW-DF2 is demonstrated in Figure 9 for Se_4-Se_4 fragments where we compare vdW-DF1 and vdW-DF2 results. The two approaches differ mainly by the model of exchange they use (rPW86 vs revPBE). E_{int} is now different in the two models, and hence exchange makes a contribution to the bias. Adding a fraction of semilocal GC correction ($a_c = 0.5$) has qualitatively a similar effect but compared to adding exact exchange causes overbinding. In terms of the modified $E_{xc}^{0Becke3LYP'}$ functional,[55] we find a good agreement with CCSD(T) using $a_0 = 1$ and $a_c = 0$ in the noncovalent regime. More sophisticated and accurate parametrization could be found, if needed. In practice, HF exchange significantly improves the interaction curves, making them less repulsive than the original vdW-DF2 at distances

dx.doi.org/10.1021/ct300258z | J. Chem. Theory Comput. 2012, 8, 2301−2309

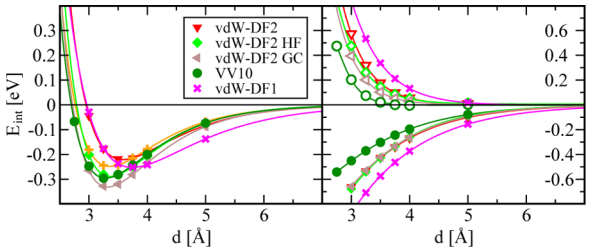

Figure 9. Interaction energies for Se_6−Se_6 fragments showing results of VV-vdW and vdW-DF theories with different models for E_{xc}^0/E_c^{nl} partitioning. Caption details as in Figures 2 and 3.

smaller than ∼4 Å. Contrarily, the more metallic Te system is more correlation dominated at short distances (≤3.5 Å) and more exchange dominated at larger distances (≥3.5 Å), and the entire PES would best be described by a split description in the two regimes. As a compromise, we show in Figure 6 a description with both exact exchange and GC corrections simultaneously added (a_0 = 0.5, a_c = 0.5).

VV-vdW describes the fragment interaction also in this group very well, and the success can be understood by comparison with our modified vdW-DF description. Adding a full GC correction to rPW86 exchange and changing E_c^{nl} results in a slightly less satisfactory agreement with CCSD(T) for the Te_6−Te_6 system, comparative quality for the Se_6−Se_6 system, and slightly improved results for S_6−S_6, compared to vdW-DF2 with exact exchange. Incidentally, we find the largest disagreement with CCSD(T) for the Te_6−Te_6 fragment, where a split HF/(modified)GC treatment is required.

In DFT-D theories, the best description results from DFT-D HP treatment, with DFT-D3 being slightly less accurate, especially for the S_6−S_6 fragment, and DFT-D2 being of mixed quality, as usual.

Trends emerge from comparison of E_{xc}^0. rPW86 in vdW-DF2 is too repulsive compared to CCSD(T); exact exchange is slightly less repulsive. Adding GC correlation makes the curve even less repulsive, while TPSS is qualitatively different. Part of these differences is built into the E_c^{nl}/E_{Disp} curves, see e.g. the differences between VV10 and vdW-DF2 or the DFT-D type of theory.

The quality of description of our database by different approximate descriptions can be characterized by *mean absolute errors* (MAE) in interaction energies (E_{int}) and equilibrium distances between fragments (d_{eq}). The MAE for our database in various treatments and approximations is shown in Figure 10. MP2 exhibits the largest deviations, i.e. overbinding, from our CCSD(T) reference data. vdW-DF2 improves significantly the overbinding but exhibits a systematic overestimation of equilibrium fragment distances. VV-vdW in the VV10 flavor exhibits overall the best agreement with CCSD(T) benchmark results, only slightly improved by our educated fitting of the short-/medium-range correlations, E_{xc}^0. From DFT-D theories, the DFT-D3 method is consistently in best agreement with CCSD(T). Again, slight improvement can be achieved by use of the Tkatchenko−Scheffler method to determine the C_6 dispersion coefficient with a reparamtrization of the dispersion tails, if needed. Slightly inferior results were obtained with the alternative E_{xc}^{nl}/E_{xc}^0 pairings, see the SI.

4. CONCLUSIONS

We have presented an extended study of interaction energies of small model vdW fragments of group VA (P, As, Se) and group

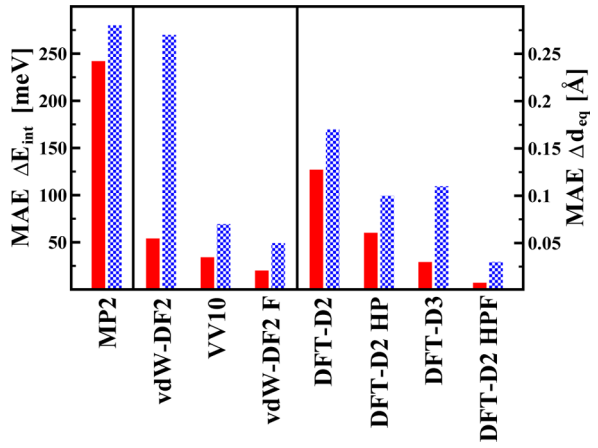

Figure 10. Mean absolute errors in interaction energies E_{int} at the minima (red bars) and in the respective equilibrium distances d_{eq} (blue bars) of different functionals and approaches with respect to our calculated CCSD(T) results. vdW-DF2 F stands for vdW-DF2 results with tuned E_{xc}^0 using physically motivated fitting.

VIA (S, Se, Te) atoms. These systems fill a gap in otherwise recently much studied systems interacting via noncovalent interactions. Quasi-exact complete basis set CCSD(T) benchmarks have been produced and compared with results obtained by DFT theory with approximate treatment of dispersion interactions, i.e., with vdW-DF, VV-vdW, and DFT-D theories. We have compared the relative merits and drawbacks of these techniques and outlined routes for their improvement based on physical insights. The simple systems considered here show a surprising diversity of behavior of their electronic properties ranging from more metallic to more insulator like, which needs to be captured in the more approximate methods.

We find that no DFT theory with approximate treatment of dispersion interactions is able to describe the interaction curves with high, i.e. with chemical or better, accuracy over a wide range of distances. Yet, high accuracy over a wide range of configuration space is required if vdW systems are used, for instance, in nanotribology, if pressure is exerted on them, if finite-temperature dynamics is attempted, and in other situations. In all of these applications, a numerically efficient and highly accurate method for treatment of vdW interactions is required. From the standard approaches tested here, the VV10 realization of the VV-vdW[20] and DFT-D3[12] theories stands out as the most accurate. DFT-D2 has a mixed, strongly system dependent performance. MP2 has a systematic trend to strong overbinding, and vdW-DF2[15] in its original form systematically underbinds and leads to longer equilibrium distances. We found that DFT methods with an approximate description of dispersion interactions can be tuned to high accuracy by (a) matching the nonlocal long-range correlation terms calculated within vdW-DF theories with DFT treatment of the short-/medium-range exchange-correlation (E_{xc}^0), therby supplying the missing parts of correlations, or (b) by careful reparatrization of the dispersion term (E_{Disp}) relative to an accurate benchmark in the more empirical DFT-D theories. Matching of a suitable E_{xc}^0 in the noncovalent regime where customary DFT xc functionals may not be optimal can be guided by physical insights, such as, for instance, by local gap densities. The challenge here is to recognize which part of E_{xc}^0 needs amendment. We have found that hybrid/semilocal functionals provide enough flexibility for this purpose. For

example, group VA fragments are more metallic-like, hence correlation dominated, whereas group VIA fragments are more insulator-like, hence exchange dominated. P and Te represent exceptions where both contributions play a role. Due to a consistent fitting-free treatment of both E_{xc}^{0} and E_{c}^{nl}, vdW-DF theories are the best starting point for educated matching of E_{xc}^{0} with E_{c}^{nl}. When E_{Disp} in DFT-D theories is reparametrized, we found that it is useful to start from a DFT-D2 type of procedure with C_6 dispersion coefficients and vdW radii determined by the Tkatchenko−Scheffler procedure,[28] rather than trying to modify the much more complex DFT-D3 theory. Obviously, the Tkatchenko−Scheffler procedure will be especially useful if charge transfer processes are involved. Surprisingly, the same set of reparametrized coefficients appears to fix the discrepancies. In general, however, parameters of a system optimized xc hole, including E_{xc}^{0}, are unlikely to be universal and have to be determined individually for each system/group of systems at hand.

There are obviously more alternatives for the description of vdW interactions such as, for instance, SAPT-DFT,[56,57] which uses TDDFT to calculate the dispersion contribution to the binding energy. Given the $O(N^5)$ scaling with system size, finite accuracy compared to the best quantum chemistry methods and the fact that SAPT-DFT application necessitates the identification of individual fragments, we believe that there are more competitive alternatives. Beyond small finite systems, such as vdW interacting molecules and clusters, our strategy for an accurate treatment of vdW interacting extended systems also starts from a cluster model, treated by the most accurate method available: CBS CCSD(T) for smaller systems or QMC for larger systems. Since the short-/medium-range part of the xc hole converges fast with the size of the cluster model[37] and E_{Disp}/E_{c}^{nl} is essentially a pairwise interaction, which can be corrected for possible screening effects,[34,35] if appropriate, the entire xc hole will show a rapid convergence with the size of the cluster. Hence, the xc hole optimized for the finite cluster system can relatively easily be transferred to the extended system.

■ ASSOCIATED CONTENT

Supporting Information

We have also calculated PBE/TPSS coupling of the short-/medium-range correlations in DFT-D2, DFT-D3, and DFT-D2 with Hirshfeld partitioning for group VA fragments and revPBE for group VIA fragments. These results are summarized in the Supporting Information. The reason for not choosing such an otherwise standard pairing of xc functionals[6] for group VA was the presence of spurious exchange binding[14,18] and for group VIA the slightly worse results resulting from such pairings. This material is available free of charge via the Internet at http://pubs.acs.org/.

■ AUTHOR INFORMATION

Corresponding Author

*E-mail: ivan.stich@savba.sk.

Notes

The authors declare no competing financial interest.

■ ACKNOWLEDGMENTS

Financial support from APVV project APVV-ESF-0007-07 and from project VEGA 2/0007/12 is acknowledged. This research was supported in part also by ERDF OP R&D, project CE meta-QUTE ITMS 26240120022, and via CE SAS QUTE.

■ REFERENCES

(1) Parsegian, V. A. *Van der Waals Forces: A Handbook for Biologists, Chemists, Engineers, and Physicists*; Cambridge University Press: Cambridge, England, 2005.
(2) Brndiar, J.; Turanský, R.; Dietzel, D.; Schirmeisen, A.; Štich, I. *Nanotechnology* **2011**, *22*, 085704.
(3) Brndiar, J.; Turanský, R.; Štich, I. *Phys. Rev. B* **2011**, *84*, 085449.
(4) Hobza, P.; Šponer, J. *J. Am. Chem. Soc.* **2002**, *124*, 11802.
(5) Jurečka, P.; Šponer, J.; Černý, J.; Hobza, P. *Phys. Chem. Chem. Phys.* **2006**, *8*, 1985.
(6) Marom, N.; Tkatchenko, A.; Rossi, M.; Gobre, V. V.; Hod, O.; Scheffler, M.; Kronik, L. *J. Chem. Theory Comput.* **2011**, *7*, 3944.
(7) Goerigk, L.; Grimme, S. *J. Chem. Theory Comput.* **2010**, *6*, 107.
(8) Runeberg, N.; Pyykkö, P. *Int. J. Quantum Chem.* **1998**, *66*, 131.
(9) Grimme, S.; Mück-Lichtenfeld, C.; Antony, J. *J. Phys. Chem. C* **2007**, *111*, 11199.
(10) Chakarova-Käck, S. D.; Schröder, E.; Lundqvist, B. I.; Langreth, D. C. *Phys. Rev. Lett.* **2006**, *96*, 146107.
(11) Moses, P. G.; Mortensen, J. J.; Lundqvist, B. I.; Nørskov, J. K. *J. Chem. Phys.* **2009**, *130*, 104709.
(12) Grimme, S.; Anony, J.; Ehrlich, S.; Krieg, H. *J. Chem. Phys.* **2010**, *132*, 154104.
(13) Pernal, K.; Podeszwa, R.; Patkowski, K.; Szalewicz, K. *Phys. Rev. Lett.* **2009**, *103*, 263201.
(14) Dion, M.; Rydberg, H.; Schröder, E.; Langreth, D. C. *Phys. Rev. Lett.* **2004**, *92*, 246401.
(15) Lee, K.; Murray, E. D.; Kong, L.; Lundqvist, B. I.; Langreth, D. C. *Phys. Rev. B* **2010**, *82*, 081101(R).
(16) Vydrov, O. A.; Van Voorhis, T. *J. Chem. Phys.* **2009**, *131*, 019904.
(17) Perdew, J. P.; Yue, W. *Phys. Rev. B* **1986**, *33*, 8800(R).
(18) Murray, E. D.; Lee, K.; Langreth, D. C. *J. Chem. Theory Comput.* **2009**, *5*, 2754.
(19) Klimeš, J.; Bowler, D. R.; Michaelides, A. *J. Phys.: Condens. Matter* **2010**, *22*, 022201.
(20) Vydrov, O. A.; Van Voorhis, T. *J. Chem. Phys.* **2010**, *133*, 244103.
(21) Vydrov, O. A.; Van Voorhis, T. *Phys. Rev. Lett.* **2009**, *103*, 063004.
(22) Grimme, S. *J. Comput. Chem.* **2004**, *25*, 1463.
(23) Grimme, S. *J. Comput. Chem.* **2006**, *27*, 1787.
(24) Schwabe, T.; Grimme, S. *Phys. Chem. Chem. Phys.* **2007**, *9*, 3397.
(25) Becke, A. D. *J. Chem. Phys.* **1997**, *107*, 8554.
(26) Tao, J.; Perdew, J. P.; Staroverov, V. N.; Scuseria, G. *Phys. Rev. Lett.* **2003**, *91*, 146401.
(27) Perdew, J. P.; Tao, J.; Staroverov, V. N.; Scuseria, G. *J. Chem. Phys.* **2004**, *120*, 6898.
(28) Tkatchenko, A.; Scheffler, M. *Phys. Rev. Lett.* **2009**, *102*, 073005.
(29) Perdew, J. P.; Burke, K.; Ernzerhof, M. *Phys. Rev. Lett.* **1996**, *77*, 3865.
(30) Perdew, J. P.; Burke, K.; Ernzerhof, M. *Phys. Rev. Lett.* **1997**, *78*, 1396.
(31) Ernzerhof, M.; Scuseria, G. E. *J. Chem. Phys.* **1999**, *110*, 5029.
(32) Adamo, C.; Scuseria, G. E. *J. Chem. Phys.* **1999**, *111*, 2889.
(33) Heyd, J.; Scuseria, G. E.; Ernzerhof, M. *J. Chem. Phys.* **2003**, *118*, 8207.
(34) Ruiz, V. G.; Liu, W.; Zojer, E.; Scheffler, M.; Tkatchenko, A. *Phys. Rev. Lett.* **2012**, *108*, 146103.
(35) Zhang, G.-X.; Tkatchenko, A.; Paier, J.; Appel, H.; Scheffler, M. *Phys. Rev. Lett.* **2011**, *107*, 245501.
(36) Deligkarisz, C.; Rodriguez, J. H. *Phys. Chem. Chem. Phys.* **2012**, *14*, 3414.
(37) Hu, Q.-M.; Reuter, K.; Scheffler, M. *Phys. Rev. Lett.* **2007**, *98*, 176103.
(38) Perdew, J. P.; Chevary, J. A.; Vosko, S. H.; Jackson, K. A.; Pederson, M. R.; Singh, D. J.; Fiolhais, C. *Phys. Rev. B* **1992**, *36*, 6671.

(39) Burkatzki, M.; Filippi, C.; Dolg, M. *J. Chem. Phys.* **2008**, *126*, 234105.
(40) Dunning, T. H. *J. Chem. Phys.* **1989**, *90*, 1007.
(41) Schmidt, M. W.; Baldridge, K. K.; Boatz, J. A.; Elbert, S. T.; Gordon, M. S.; Jensen, J. H.; Koseki, S.; Matsunaga, N.; Nguyen, K. A.; Su, S.; et al. *J. Comput. Chem.* **1993**, *14*, 1347. For code, see www.msg.ameslab.gov/gamess/ (accessed Jun. 2012).
(42) Boys, S. F.; Bernardi, F. *Mol. Phys.* **2002**, *100*, 65.
(43) Halkier, A.; Helgaker, T.; Jorgensen, P.; Klopper, W.; Olsen, J. *Chem. Phys. Lett.* **1998**, *294*, 45.
(44) Halkier, A.; Helgaker, T.; Jorgensen, P. *Chem. Phys. Lett.* **1999**, *302*, 437.
(45) Schuchardt, K. L.; Didier, B. T.; Elsethagen, T.; Sun, L.; Gurumoorthi, V.; Chase, J.; Li, J.; Windus, T. L. *J. Chem. Inf. Model.* **2007**, *47*, 1045.
(46) Štich, I. *Acta Phys. Slov.* **2007**, *57*, 1.
(47) Vanderbilt, D. *Phys. Rev. B* **1990**, *41*, 7892.
(48) Zhang, Y.; W., W. *Phys. Rev. Lett.* **1998**, *80*, 890.
(49) Marx, D.; Hutter, J. In *Modern Methods and Algorithms of Quantum Chemistry*; Grotendorst, J., Ed.; FZ Jülich, NIC: Jülich, Germany, 2000. For code, see www.cpmd.org (accessed Jun. 2012).
(50) Troullier, N.; Martins, J. L. *Phys. Rev. B* **1991**, *43*, 1993.
(51) For code, see www.quantum-espresso.org (accessed Jun. 2012).
(52) For code, see www.thch.uni-bonn.de/tc/orca/ (accessed Jun. 2012).
(53) Chu, X.; Dalgarno, A. *J. Chem. Phys.* **2004**, *121*, 4083.
(54) Tran, F.; Blaha, P. *Phys. Rev. Lett.* **2009**, *102*, 226401.
(55) Becke, A. D. *J. Chem. Phys.* **1993**, *98*, 5648.
(56) Misquitta, A. J.; Jeziorski, B.; Szalewicz, K. *Phys. Rev. Lett.* **2003**, *91*, 033201.
(57) Podeszwa, R.; Szalewicz, K. *Chem. Phys. Lett.* **2005**, *412*, 488.